AMERICAN ACADEMY OF OPHTHALMOLOGY®

Unfolding the Pitchfork Sign in Type 2 Choroidal Neovascularization: A Longitudinal Analysis and 3-Dimensional Reconstructions

Edoardo Balduzzi, MD,[1,2] *Giovanni Ometto, PhD,*[3,4] *Francesco Bandello, MD,*[1,2] *Elisabetta Miserocchi, MD,*[1,2] *Maria Vittoria Cicinelli, MD*[1,2]

Purpose: To longitudinally characterize and redefine the structural basis and clinical significance of the pitchfork sign in type 2 choroidal neovascularization (CNV) using multimodal imaging with 3-dimensional confirmation.

Design: Retrospective observational study.

Subjects: Thirty-nine eyes with treatment-naive type 2 CNV showing a pitchfork sign on spectral-domain OCT.

Methods: Outer retinal changes were graded, focusing on splitting at the ellipsoid zone (EZ) and infolding of the external limiting membrane (ELM). Quantitative measures included projection number, maximal fold height, subretinal fluid (SRF) height, subretinal hyperreflective material (SHRM) height, and posttreatment pigment epithelial detachment (PED) height; correlations with best-corrected visual acuity (BCVA) (logarithm of the minimum angle of resolution) were assessed. Three-dimensional reconstructions of the outer retina were generated to verify the spatial configuration of folds.

Main Outcome Measures: Structural characterization of the retinal layer involved in the pitchfork sign; quantitative morphologic parameters (projection number and maximal fold height); their correlation with exudative and anatomical features (SRF, SHRM, PED height); and association with BCVA.

Results: The pitchfork sign occurred in idiopathic (69%), inflammatory (23%), and myopic (8%) CNV, indicating it is not disease-specific. Imaging revealed a reproducible mechanical sequence: elevation of the outer retina by type 2 CNV; cleavage at the EZ with formation of a new fluid-filled split between the EZ and ELM; centrifugal buckling and infolding from the lesion margin toward the CNV core; and, in some eyes, transient partially enclosed "mushroom-shaped" closed folds that trapped fluid. These folds ultimately collapsed into sharply angulated vertical hyperreflective lines—the pitchfork configuration. Three-dimensional reconstructions confirmed that the apparent "tines" are radially arranged outer retinal folds anchored to the neovascular complex. Quantitatively, fold number correlated with SRF height ($r = 0.40$, $P = 0.01$), SHRM height ($r = 0.41$, $P = 0.009$), and maximal fold height ($r = 0.49$, $P = 0.002$). Greater maximal fold height was associated with worse presenting BCVA ($r = 0.48$, $P = 0.003$). After anti-VEGF, all folds resolved, and the CNV regressed beneath a continuous retinal pigment epithelium, forming a fibrovascular PED whose height at follow-up correlated with baseline fold count ($r = 0.35$, $P = 0.04$).

Conclusions: The pitchfork sign in type 2 CNV reflects transient, mechanically induced folding and splitting of the outer retina overlying subretinal neovascular tissue, rather than an inflammatory biomarker. Greater retinal deformation at presentation was associated with worse presenting vision and with a higher fibrovascular PED after treatment.

Financial Disclosure(s): Proprietary or commercial disclosure may be found in the Footnotes and Disclosures at the end of this article. *Ophthalmology Science 2026;6:101200*

Supplemental material available at www.ophthalmologyscience.org.

The pitchfork sign is a characteristic OCT pattern described in choroidal neovascularization (CNV), consisting of multiple tapered, finger-like hyperreflective projections arising from the subretinal neovascular complex and extending toward or across the external limiting membrane (ELM) and ellipsoid zone (EZ).[1,2] Since its original description, it has been widely regarded as a hallmark of inflammatory CNV and is frequently cited as a diagnostic feature distinguishing inflammatory from degenerative type 2 CNV.[3–6]

Despite its widespread recognition, the structural substrate and pathophysiologic basis of the pitchfork sign remain incompletely understood. Its interpretation as an inflammatory biomarker largely derives from early case series rather than systematic morphologic or longitudinal analyses.[1,2] With advances in high-resolution structural

http://doi.org/10.1016/j.xops.2026.101200
ISSN 2666-9145/26

OCT, en face reconstruction, and OCT angiography (OCTA), pitchfork-like projections have increasingly been identified in type 2 or mixed CNV unrelated to uveitis, including idiopathic and peripapillary lesions.[7,8] These observations challenge the assumption that the sign is disease-specific and suggest that it may reflect a more general morphologic response of the outer retina to subretinal pathology.

Emerging imaging data support a mechanical interpretation. Falavarjani et al,[8] using en face OCT, demonstrated a radial or wreath-like arrangement of spikes surrounding the neovascular complex and reported their regression after anti-VEGF therapy. The absence of intrinsic flow signal within these projections on OCTA further argued against a vascular origin. Collectively, these findings raise the possibility that the pitchfork sign represents a dynamic structural deformation of the outer retina induced by subretinal neovascular growth, rather than a fixed inflammatory fingerprint.

Building on these observations, the present study aims to further elucidate the proposed structural basis of the pitchfork sign using 3-dimensional (3D) OCT volume reconstruction in treatment-naïve type 2 CNV. Specifically, we sought to characterize the spatial relationship between outer retinal deformation and the underlying neovascular complex, quantify morphologic correlates, evaluate reversibility following anti-VEGF therapy, and examine associations with anatomical and functional outcomes. By integrating cross-sectional, en face, and volumetric analyses, we aim to refine the mechanistic interpretation of the pitchfork sign and reassess its long-standing classification as a disease-specific inflammatory marker.

Methods

This retrospective observational study included consecutive eyes with treatment-naïve type 2 or mixed CNV evaluated at the San Raffaele Scientific Institute between 2015 and 2025. Type 2 lesions were selected because the neovascular complex lies above the retinal pigment epithelium (RPE) in the subretinal space, where it directly contacts and deforms the outer retina, producing the vertical protrusions that define the pitchfork sign. Mixed type 1/type 2 lesions were included when a subretinal (type 2) component was clearly visualized on structural or en face OCT. The study adhered to the tenets of the Declaration of Helsinki and was approved by the local Institutional Review Board, with a waiver of informed consent for retrospective chart review.

Eligible eyes were required to have active, treatment-naïve type 2 or mixed CNV confirmed by multimodal imaging and high-resolution structural OCT demonstrating features consistent with the pitchfork sign—defined as vertically oriented or arcuate hyperreflective projections extending from the outer retina, with or without associated subretinal fluid (SRF).[1,2]

Eyes were excluded if they showed extensive subretinal fibrosis, macular outer retinal atrophy, or significant epiretinal membrane causing retinal distortion or stiffness that could confound the evaluation of outer retinal folding. Additional exclusion criteria included poor image quality precluding reliable segmentation, prior intraocular surgery within 6 months (other than uncomplicated cataract extraction), concurrent macular diseases such as diabetic macular edema or retinal vein occlusion, and previous intravitreal therapy or photodynamic treatment.

Imaging Protocol and Qualitative Analysis

At baseline and follow-up, all eyes underwent a complete ophthalmic examination, including best-corrected visual acuity (BCVA) (converted to logarithm of the minimum angle of resolution) and multimodal imaging. Imaging included structural spectral-domain OCT, en face OCT, and OCTA when available. Baseline data included underlying disease etiology, BCVA at presentation, and BCVA at the last follow-up visit. The number of anti-VEGF agent injections administered during the study period was recorded.

Structural OCT scans were reviewed to assess CNV type (type 2 or mixed type 1/type 2), CNV location (subfoveal, extrafoveal, or peripapillary), presence of SRF or intraretinal fluid, and characteristics of inner (inner retinal wrinkling) and outer retinal layers (including splitting between the outer nuclear layer [ONL], the ELM, and the EZ).

Three-dimensional reconstruction of the outer retina was successfully performed in 5 eyes selected for optimal image quality and reliable layer segmentation. This analysis was restricted to a subset of cases because accurate volumetric reconstruction requires high-density OCT acquisition, preserved outer retinal signal, and continuous, artifact-free segmentation across the full lesion extent. In scans not meeting these criteria, volumetric reconstruction was not performed to avoid segmentation-related distortion.

En face OCT slabs were segmented at the level of the ELM to evaluate the topographic distribution and horizontal configuration of the pitchfork sign. Three-dimensional reconstructions were generated using the Volume Segmenter application in MATLAB (version R2023B; MathWorks). Segmentation boundaries were defined between the ELM and the inner border of the ONL, using manufacturer-provided scaling to preserve geometric accuracy. Within each OCT volume, the hyperreflective folded structures corresponding to the pitchfork projections were manually segmented to delineate their spatial extent.

Quantitative Analysis

Quantitative morphologic parameters were extracted from baseline structural spectral-domain OCT scans. When present, the maximum height of SRF and subretinal hyperreflective material (SHRM) was measured on the B-scan demonstrating the greatest vertical extent. Maximum fold height was defined as the perpendicular distance from the base of the neovascular complex to the apex of the corresponding hyperreflective projection. The number of outer retinal projections was independently counted by 2 masked graders. Discrepancies were resolved through joint review to achieve consensus regarding fold boundaries and projection count.

Subfoveal choroidal thickness was measured perpendicularly from the outer border of the retinal pigment epithelium to the inner scleral boundary beneath the foveal center. On follow-up OCT scans, the maximum height of the fibrovascular pigment epithelial detachment (PED) was measured at the location corresponding to the original neovascular complex.

Statistical Analysis

All statistical analyses were performed using R (version 4.3.3; R Foundation for Statistical Computing). Continuous variables were reported as mean ± standard deviation or median [range], as appropriate based on distributional characteristics. Categorical variables were summarized as absolute frequencies and percentages.

Table 1. Demographic, Morphologic, and Functional Characteristics of Eyes with Type 2 CNV Exhibiting the Pitchfork Sign across Age Subgroups

	T1 (Young) (n = 13 Eyes)	T2 (Middle) (n = 13 Eyes)	T3 (Older) (n = 13 Eyes)	Overall (N = 39 Eyes)
Age (yrs)	25.8 (9.54)	59.9 (12.1)	81.5 (4.86)	55.7 (25.0)
Female gender (%)	9 (69.2%)	8 (61.5%)	4 (30.8%)	21 (53.8%)
SCT (microns)	376 (82.5)	262 (101)	233 (100)	290 (112)
Cause				
Inflammatory	6 (46.2%)	2 (15.4%)	1 (7.7%)	9 (23.1%)
Myopic	0 (0%)	3 (23.1%)	0 (0%)	3 (7.7%)
Idiopathic	7 (53.8%)	8 (61.5%)	12 (92.3%)	27 (69.2%)
Location				
Foveal	6 (46.2%)	9 (69.2%)	7 (53.8%)	22 (56.4%)
Extrafoveal	5 (38.5%)	3 (23.1%)	4 (30.8%)	12 (30.8%)
Peripapillary	2 (15.4%)	1 (7.7%)	2 (15.4%)	5 (12.8%)
Hemorrhages	7 (53.8%)	11 (84.6%)	12 (92.3%)	30 (76.9%)
Inner wrinkling	9 (69.2%)	8 (61.5%)	10 (76.9%)	27 (69.2%)
Outer layers splitting	13 (100%)	12 (92.3%)	13 (100%)	38 (97.4%)
SHRM	9 (69.2%)	11 (84.6%)	11 (84.6%)	31 (79.5%)
SHRM height (microns)	218 (149)	256 (214)	232 (118)	235 (161)
SRF	11 (84.6%)	13 (100%)	13 (100%)	37 (94.9%)
SRF height (microns)	129 (91.4)	187 (167)	159 (86.8)	159 (120)
Tines number	4.9 (3.4)	4.2 (2.1)	3.5 (1.2)	4.2 (2.4)
Max fold height (microns)	144 (61.1)	182 (118)	140 (50.0)	155 (82.0)
Mushroom cap shape	1 (7.7%)	3 (23.1%)	1 (7.7%)	5 (12.8%)
Baseline BCVA (LogMAR)	0.312 (0.369)	0.774 (0.715)	0.449 (0.335)	0.523 (0.544)
Final BCVA baseline (LogMAR)	0.050 (0.094)	0.345 (0.515)	0.343 (0.318)	0.243 (0.379)
Anti-VEGF agent injections	1.7 (0.9)	2.7 (0.7)	2.6 (0.9)	2.3 (0.9)

BCVA = best-corrected visual acuity; CNV = choroidal neovascularization; LogMAR = logarithm of the minimum angle of resolution; SCT = subfoveal choroidal thickness; SHRM = subretinal hyperreflective material; SRF = subretinal fluid.
Data are presented as mean (standard deviation) or absolute and relative frequencies.
The cohort was divided into 3 age tertiles: **T1 (young)**, **T2 (middle-aged)**, and **T3 (older)**, each including 13 eyes, for a total of 39 eyes.
Variables include demographics, lesion etiology, location, presence of hemorrhage, inner retinal wrinkling, outer retinal splitting, SHRM, and SRF characteristics, fold parameters (number of tines and maximal fold height), and visual outcomes (baseline and final BCVA).
Comparisons show consistent expression of outer retinal folds across all age groups, with complete resolution after anti-VEGF therapy.

To investigate structural correlates of the pitchfork sign, the number of outer retinal projections was log-transformed to improve normality and stabilize variance. Associations between the log-transformed projection count and quantitative OCT parameters—including SRF height, SHRM height, maximum fold height, and posttreatment PED height—were evaluated using Pearson correlation coefficients. All tests were 2-tailed, and a P value <0.05 was considered statistically significant.

Results

Thirty-nine eyes from 39 patients with a recognizable pitchfork sign were included. The mean age at presentation was 55.7 ± 25.0 years (range, 11−84), and 21 patients (54%) were female; female predominance was greater in younger patients and declined with age. Seventeen right and 22 left eyes were affected. All cases were unilateral, treatment-naïve, and showed active CNV at presentation.

Underlying etiologies were idiopathic in 27 eyes (69%), inflammatory in 9 eyes (23%), and myopic in 3 eyes (8%). One idiopathic case had multifocal vitelliform lesions with negative genetic testing. Etiologic distribution varied by age: inflammatory CNV predominated in younger patients (46%) and declined with age, idiopathic CNV was most common in older groups (92%), and myopic CNV occurred only in the middle age tertile (23%).

Lesion location was subfoveal in 23 eyes (56%), extrafoveal in 12 (31%), and peripapillary in 5 (13%). Subretinal hemorrhage was present in 30 eyes (77%), increasing with age, and inner retinal wrinkling in 27 (69%) eyes. At baseline, a shallow fibrovascular PED adjacent to the active type 2 CNV was observed in 3 eyes (8%), corresponding to a coexisting type 1 CNV component. Fundus autofluorescence and dye angiography showed no pattern specifically corresponding to the pitchfork area (Table 1).

OCT Features

Outside the lesion, the RPE was flat and continuous; over the CNV, it was focally discontinuous with choroidal hypertransmission. The surrounding RPE was often thickened and partially draped over the neovascular complex; in 2 eyes (5%), there was no lateral RPE coverage. Subretinal hyperreflective material occupied the subretinal space in 80% of eyes, consistent with blood, exudation, and neovascular tissue, with similar height and frequency across age groups (Table 1 and Fig 1).

Subretinal fluid was present in all eyes, typically confined to the edges of the CNV lesion. Notably, the

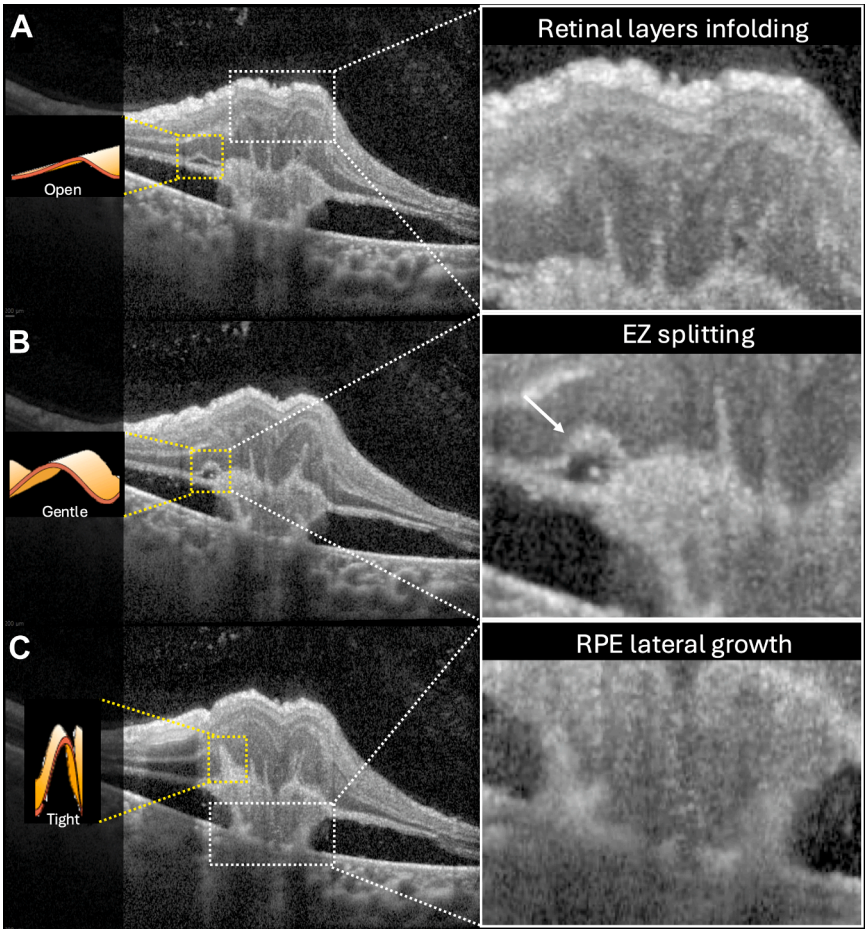

Figure 1. Structural OCT features of the pitchfork sign in active type 2 CNV. Three consecutive B-scans from the same eye show the emergence of the pitchfork sign at the center and along the margins of a type 2 CNV. The yellow boxes highlight the same outer retinal folding across adjacent sections, with separation occurring at the EZ level and a diverging, wave-like configuration that widens toward the periphery. Depending on fold width and angulation, the tines appear open (broad triangular lift), gentle (low-amplitude buckling), tight (steep, sharply angulated infolding), or close (near apposition of opposing EZ surfaces). Magnified insets on the right illustrate key mechanical correlates: **(A)** the outer retina overlying the CNV (external limiting membrane/outer nuclear layer) is indented and undulated, consistent with outer layers infolding; **(B)** a fluid-filled split is visible at the EZ level; **(C)** at the lesion edge, the RPE is focally thickened, elevated, and draped over the neovascular tissue. CNV = choroidal neovascularization; EZ = ellipsoid zone; RPE = retinal pigment epithelium.

central core of the CNV remained in direct apposition to the overlying outer retina even when SRF was present at its lateral margins.

Outer retinal splitting was observed in 98% of eyes and was most pronounced along the lateral CNV borders (Figs 2 and 3), propagating centrifugally in a zipper-like fashion. The cleavage occurred within the photoreceptor layer at the EZ, separating it from the overlying ELM; the ELM remained adherent to the ONL and buckled inward. Within the hyporeflective cleft, thin hyperreflective elements continuous with the EZ likely represented suspended debris/condensed photoreceptor material and showed no OCTA flow except in one case.

Pitchfork Sign Morphology

Analysis of consecutive transverse OCT B-scans showed that the outer retinal abnormalities underlying the pitchfork sign were present across adjacent sections but changed configuration depending on scan position. Near the center of the CNV lesion, the projections appeared narrow and steep. In more peripheral scans, they became broader and flatter. Importantly, the same projection changed width and contour across sequential B-scans, indicating that the apparent "spikes" were not separate intraretinal structures but different cross-sectional views of a continuous outer retinal fold (ORF).

To facilitate description of this behavior on two-dimensional OCT, we referred to 4 recurring appearances—open, gentle, tight, and close—based on relative width and angulation (Figs 1–3); these terms are purely descriptive and are not intended to define a classification or staging system, but rather to aid visualization of a single spatial phenomenon.

On cross-sectional OCT, the pitchfork sign appeared as vertically oriented hyperreflective projections extending from the CNV into the ONL. These projections were usually linear and occasionally arcuate, without involvement of

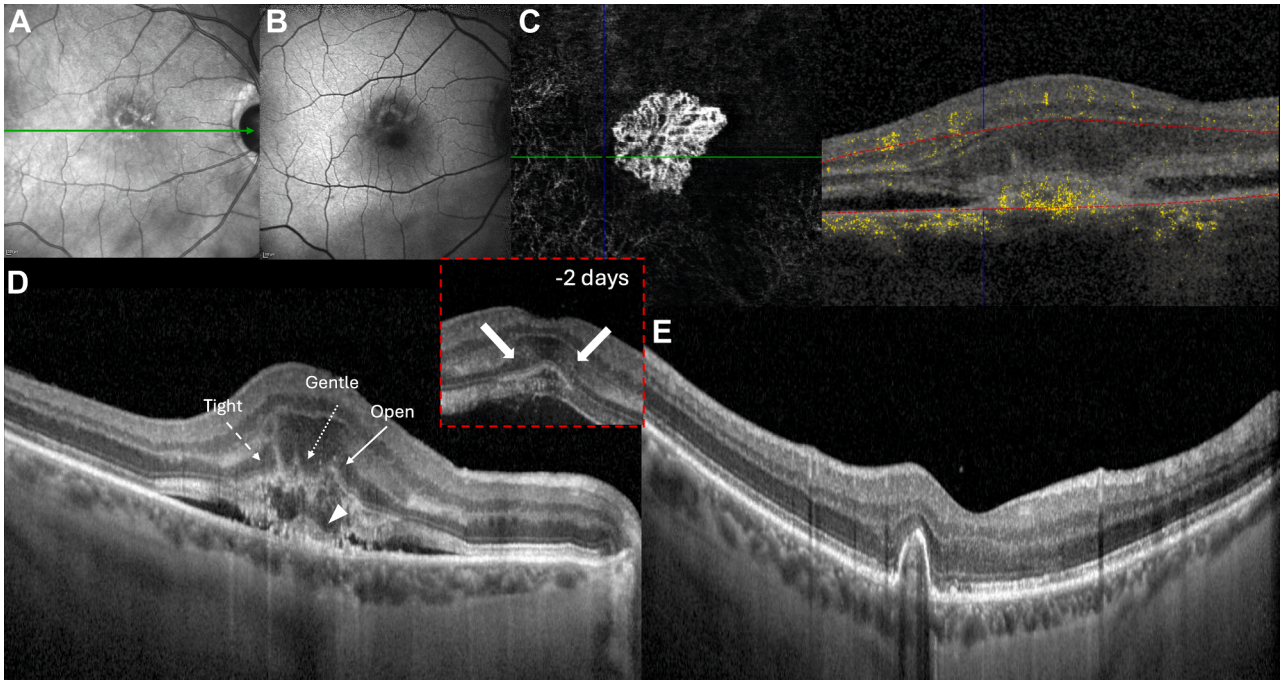

Figure 2. Outer retinal splitting and folding process in type 2 CNV. **A,** The lesion appears as a hyperreflective ring on near-infrared reflectance; **B,** it is hyperautofluorescent on blue autofluorescence. **C,** OCT angiography confirms a type 2 neovascular network; orthogonal B-scans with flow overlay demonstrate flow confined to the outer retinal hyperreflective lesion and no detectable flow above or adjacent to the CNV. **D,** A horizontal OCT highlights marked outer retinal elevation and outward bending, with a distinct split at the EZ over the CNV (white rectangle). Along the lateral borders of the lesion, a cleavage opens within the photoreceptor layer at the EZ, separating it from the overlying ELM (arrowhead); the ELM remains adherent to the ONL and buckles inward. This split propagates centrifugally in a zipper-like fashion, and the accompanying infolding at the EZ exhibits gentle, tight, and closed configurations. Subretinal fluid is confined to the lesion margins, while the CNV core remains directly apposed to the overlying outer retina, where fluid accumulates between the EZ split. The red-framed inset shows the same scan acquired 2 days earlier, capturing the emerging EZ split and an early ELM fold. **E,** At follow-up, the neovascular complex has regressed beneath a continuous RPE layer, with complete reapposition and flattening of the outer retina. CNV = choroidal neovascularization; EZ = ellipsoid zone; ELM = external limiting membrane; ONL = outer nuclear layer.

the outer plexiform layer. They originated at the level of the EZ and often appeared as paired or duplicated EZ lines where 2 surfaces of a folded outer retina came into close contact.

In 5 eyes, we observed a large outer retinal fold that entrapped SRF and assumed a mushroom-like configuration on cross-sectional OCT (Fig 4). In these cases, consecutive scans revealed different possible folding configurations. These included the classic pitchfork appearance with multiple arcuate vertical elements, a T-shaped configuration characterized by a single vertical element capped by a short horizontal arm, and, in some cases, a single vertical hyperreflective line.

Three-Dimensional Reconstructions

In the reconstructed eyes, segmentation between the ELM and the inner boundary of the ONL revealed a complex, nonplanar outer retinal architecture centered on the CNV complex. The reconstructed surface demonstrated contiguous elevations extending centrifugally from the lesion core, anchored at their base to the CNV, and progressively changing in width and orientation toward the periphery.

This volumetric view directly explained the appearance seen on cross-sectional OCT. The projections that appeared narrow and steep in central B-scans and broader in peripheral scans represented different sectional views of the same continuous ORF. They did not correspond to discrete intraretinal structures.

Overall, 3D reconstruction provided spatial evidence that the pitchfork sign represents outer retinal folding overlying the CNV complex, clarifying its structural basis (Fig 5).

Follow-Up and Functional Correlations

The number of tines was positively correlated with SRF height ($r = 0.40$, $P = 0.01$), SHRM height ($r = 0.41$, $P = 0.009$), and maximal tine height ($r = 0.49$, $P = 0.002$). Its association with baseline BCVA in logarithm of the minimum angle of resolution units was weaker and not statistically significant ($r = 0.26$, $P = 0.1$). However, worse presenting vision (higher logarithm of the minimum angle of resolution) correlated with greater SRF height ($r = 0.51$, $P = 0.002$), greater SHRM height ($r = 0.66$, $P < 0.001$), and higher maximal fold height ($r = 0.48$, $P = 0.003$). Together, these relationships suggest that more exudation

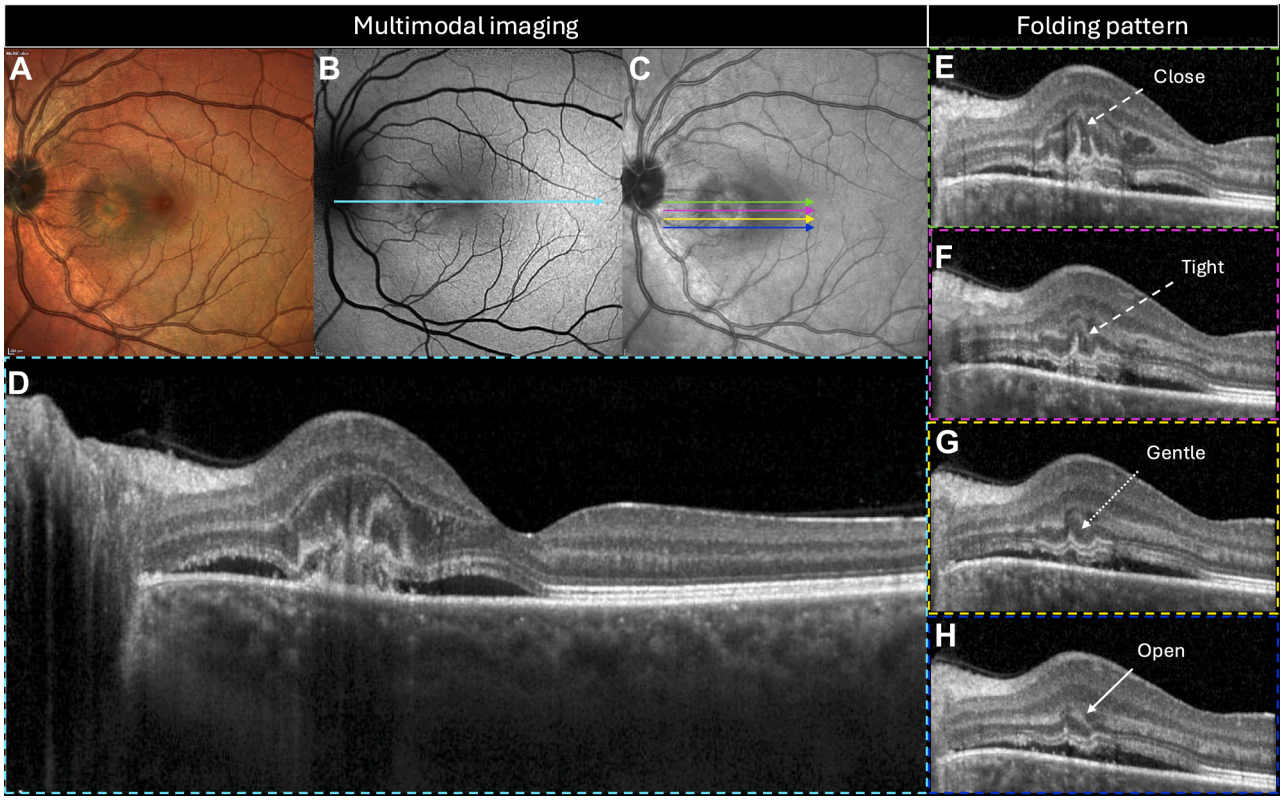

Figure 3. Centrifugal "unfolding" of the pitchfork sign. Multicolor imaging of a patient with type 2 CNV shows a circular pigmented area in the nasal parafovea **(A)**, mildly hyperautofluorescent on fundus autofluorescence **(B)**, and hyperreflective on near-infrared reflectance **(C)**. A horizontal OCT through the center of the CNV lesion **(D)** demonstrates subretinal hyperreflective material with posterior shadowing and perilesional subretinal fluid. The overlying outer retina is sharply angulated into tight, vertically oriented folds, producing the pitchfork configuration **(E)**. Sequential, adjacent OCT scans **(E–H)** depict a centrifugal gradient in fold geometry: near the CNV core, the folds are steep and closed; moving peripherally, they progressively "unfold," becoming more open as the ellipsoid zone/external limiting membrane split widens and the outer retina infolds with lower angulation. CNV = choroidal neovascularization.

and greater outer retinal deformation at baseline are associated with both a higher fold burden and poorer visual acuity.

Follow-up imaging was available in 34/39 eyes (85%); the first posttreatment visit occurred after 110.3 ± 71.0 days with a mean of 2.31 ± 0.90 anti-VEGF injections. The pitchfork sign was absent in all eyes at the first follow-up. On OCT, the type 2 CNV had regressed beneath a newly formed fibrovascular PED in 31 eyes (91%), with no residual SRF/intraretinal fluid. Pigment epithelial detachment height at follow-up correlated with baseline fold number ($r = 0.35$, $P = 0.04$), worse presenting BCVA ($r = 0.51$, $P = 0.003$), SRF height ($r = 0.78$, $P < 0.0001$), SHRM height ($r = 0.84$, $P < 0.0001$), and maximal fold height ($r = 0.63$, $P < 0.001$) (Fig S1, available at www.ophthalmologyscience.org).

Discussion

In this multimodal imaging study of 39 eyes with treatment-naïve type 2 CNV, we investigated the structural basis and clinical course of the pitchfork sign. Four principal findings emerged. First, the sign was not confined to inflammatory etiologies and was most frequently observed in idiopathic and myopic CNV without clinical or angiographic evidence of active inflammation. Second, structural OCT and 3D reconstructions demonstrated that the pitchfork sign represents folding of the outer retina overlying subretinal neovascular tissue. Third, the number and height of the outer retinal projections correlated with the degree of subretinal exudation, supporting a mechanically driven process. Finally, the sign disappeared rapidly after anti-VEGF therapy, indicating that it reflects a reversible structural deformation rather than inflammatory infiltration.

Type 2 CNV develops when abnormal vessels breach Bruch membrane and the RPE and proliferate in the subretinal space as a fibrovascular sheet.[9,10] This "subneurosensory" growth pattern is seen in age-related macular degeneration,[11] myopic macular degeneration,[12] angioid streaks,[13,14] and inflammatory entities such as punctate inner choroidopathy and multifocal choroiditis.[15] The pitchfork sign was first described by Hoang et al[1] in young patients with inflammatory CNV as vertically oriented, tapered hyperreflective projections extending from the

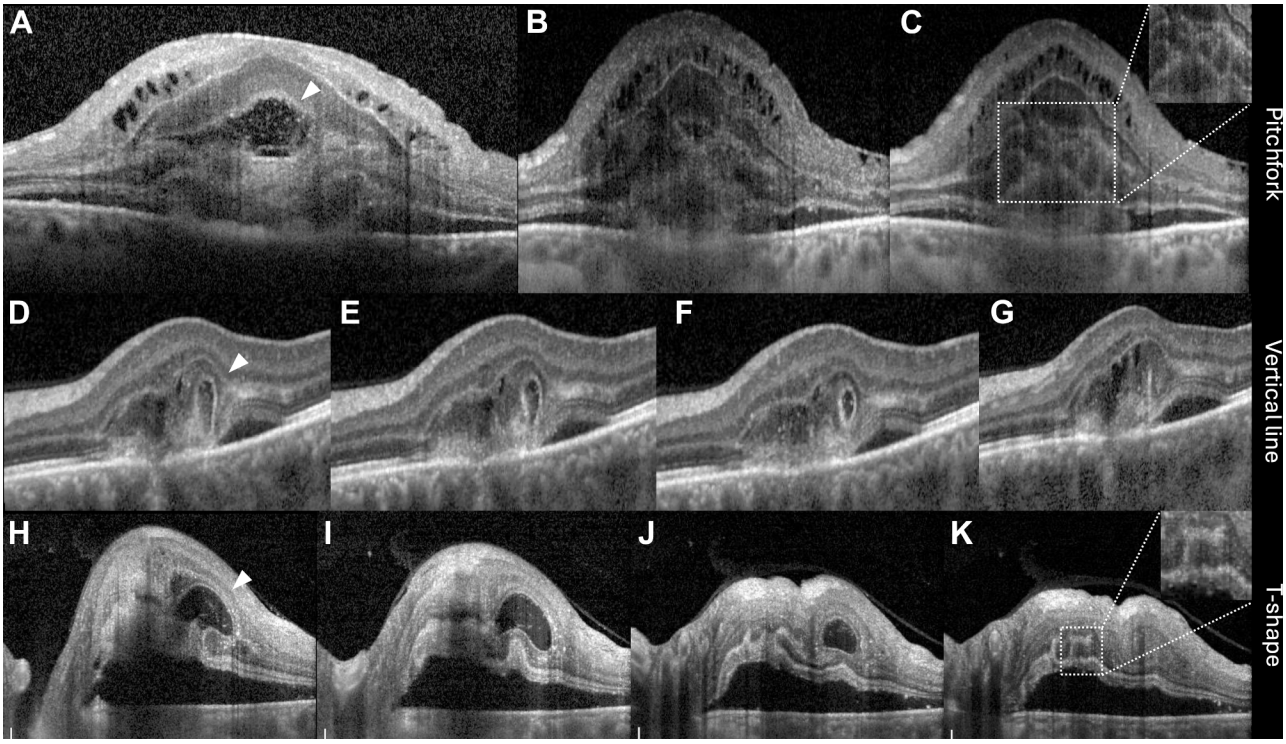

Figure 4. Different folding patterns in type 2 choroidal neovascularization. Representative examples from 3 eyes demonstrating a large, transient outer retinal fold with a mushroom-like configuration. When this structure is present, the outer retina may fold in several distinct configurations. The fluid pocket, which is in continuity with the subretinal space, is indicated by arrowheads. Consecutive scans show how this space progressively becomes smaller, eventually collapsing into hyperreflective lines—the pitchfork signature. Depending on the folding axis and local shear, the final closed-fold profile assumes one of 3 recurring patterns: a tri or multipartite configuration with arcuate vertical elements **(A–C)**, a single vertically oriented line **(D–G)**, or a T-shaped profile with a vertical stem capped by 2 short horizontal arms **(H–K)**. Note the opposing fold walls forming a partially enclosed, fluid-filled lumen, producing a "mushroom cap" configuration.

lesion into the outer retina. It was proposed to reflect inflammatory or fibrinous material within the outer retina and has since been cited as a diagnostic clue favoring an inflammatory etiology over a purely degenerative one.

Our series challenges that interpretation. We observed the pitchfork sign across a range of type 2 CNV presentations, most of them noninflammatory, and without a specific correlate on fluorescein angiography, indocyanine green angiography, or fundus autofluorescence. This supports the view that the pitchfork sign is not pathognomonic for uveitis-associated CNV, but rather a structural response of the outer retina to a subretinal neovascular complex. Inflammatory disorders may show the sign more frequently because exudation and fibrovascular proliferation increase vertical traction and subretinal expansion, but inflammation is not required for the sign to appear.[4]

High-density OCT, en face reconstructions, and 3D modeling allowed direct visualization of this process, as in several other retinal diseases.[16,17] Falavarjani et al[8] described a "spiked-wreath" configuration in 5 cases of type 2 CNV, in which hyperreflective spikes on B-scan OCT corresponded to a radial array surrounding the neovascular membrane on en face OCT. Those spikes showed no detectable flow on OCTA, and SRF was consistently present. The authors proposed that the pitchfork sign represents radial folds of the outer retina induced by mechanical effects of the neovascular lesion, rather than intraretinal neovascular sprouts or inflammatory plugs.

Our analysis is consistent with, and extends, this mechanical model. The critical anatomical clarification provided by this study concerns the retinal layer involved. Inspection of two-dimensional and 3D reconstruction show that the projections originate at the level of the EZ and represent folded photoreceptor layers. The ELM remains continuous across the lesion, although locally distorted. Thus, the apparent "tines" do not represent isolated ELM strands or intraretinal inflammatory material, but rather cross-sectional views of folded outer retina.

In some eyes, we also observed partially enclosed, fluid-filled lumens within these folds, creating a mushroom-like configuration. These lumens contained hyporeflective or mildly hyperreflective material and showed no OCTA flow signal. We interpret this configuration as a temporary compartmentalization of fluid within the folded tissue. With resolution of the intraluminal fluid, the folded outer retina reapposes, leading once again to juxtaposition and apparent EZ duplication. This supports the idea that the pitchfork sign reflects mechanical deformation and compartmentalized SRF rather than active vascular proliferation within the neurosensory retina.

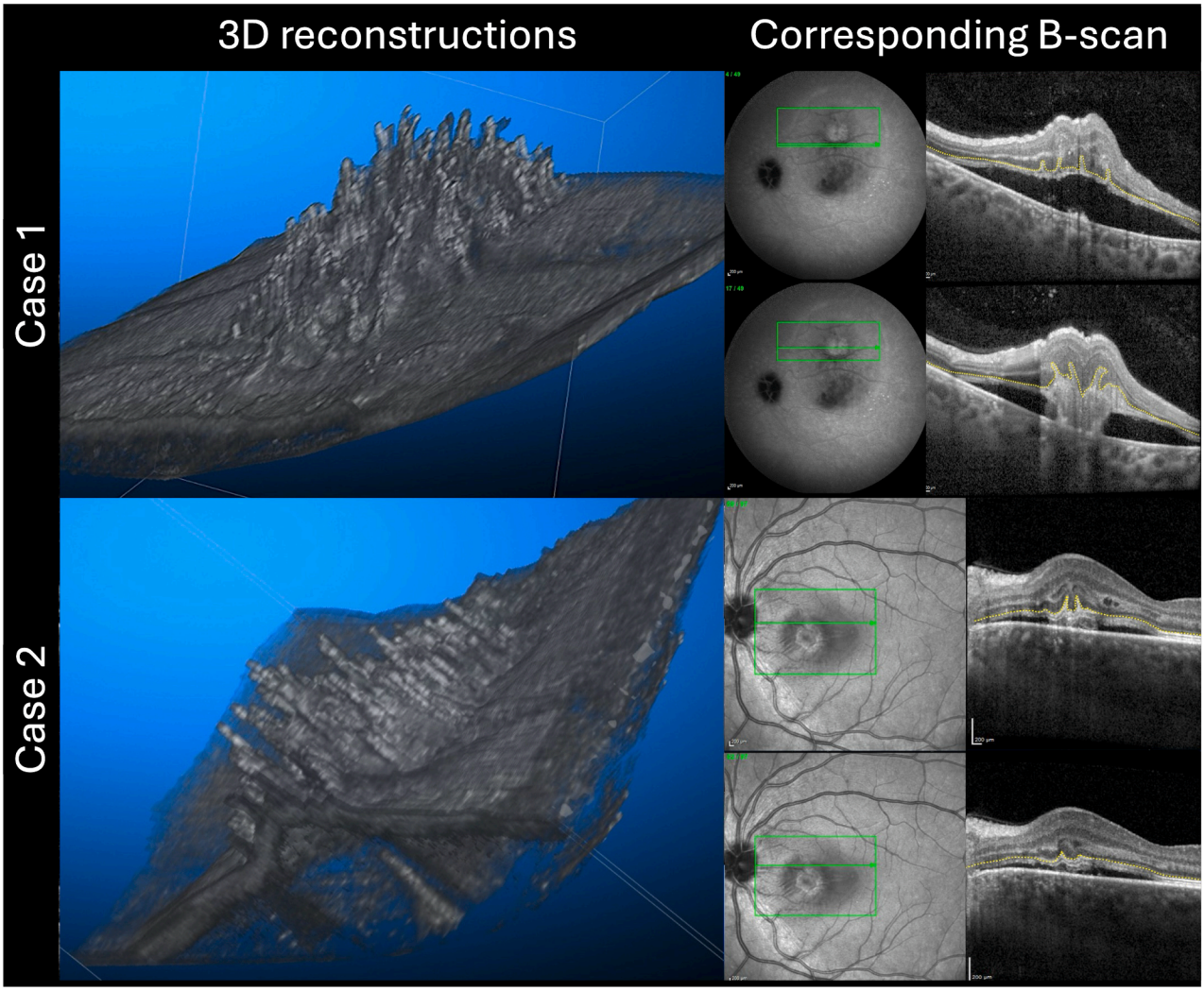

Figure 5. Three-dimensional reconstruction of outer retinal folds in 2 patients. Three-dimensional OCT reconstruction of the outer retina in 2 eyes with active type 2 CNV showing a pitchfork sign. The slab was segmented between the external limiting membrane and the inner boundary of the ONL; corresponding B-scans on the left indicate the segmentation planes. In the 3D view, the surface overlying the CNV is markedly corrugated, composed of clustered, vertically elongated ridges that arise from the CNV core and widen centrifugally toward the periphery. These ridges correspond one-to-one with the hyperreflective "tines" seen on B-scan, confirming that the pitchfork sign reflects continuous outer retinal folds rather than isolated intraretinal projections. 3D = 3-dimensional; CNV = choroidal neovascularization; ONL = outer nuclear layer.

Taken together, the structural sequence suggested by our data is as follows. The type 2 CNV elevates the overlying outer retina. Mechanical resistance at the photoreceptor—RPE interface prevents uniform displacement. A cleavage plane then opens within the photoreceptor layer at the level of the EZ, which is known to represent a mechanically vulnerable interface.[18,19] This split propagates centrifugally from the lesion margin, producing a V-shaped, fluid-filled separation between the EZ and the ELM. As exudation expands this compartment, the outer retina buckles into discrete folds. Steep, high-tension folds generate thin, linear, hyperreflective tines on OCT; broader, lower-tension folds form open, triangular separations; and when the fold walls meet at the base and then separate distally, a partially enclosed lumen with a mushroom-like appearance develops. The qualitative "open, gentle, tight, closed" configurations we observed are consistent with these different mechanical expressions.

Demographic data support the theory of a mechanical rather than inflammatory origin. Zicarelli et al[20] evaluated 185 eyes with idiopathic, myopic, or age-related macular degeneration-related type 2 CNV and found that the pitchfork sign was more common in younger patients, independent of etiology. In multivariable analysis, age—but not presumed inflammatory status—was associated with its presence. This suggests that retinal elasticity and outer retinal adhesion, which change with age, influence the retina's tendency to buckle in response to a type 2 CNV. Our cohort similarly showed the sign in younger idiopathic lesions, not only in clinically inflamed eyes.

The same mechanical ingredients appear in ORFs described after rhegmatogenous retinal detachment repair[21,22] or after serous detachments without CNV.[5,23] In those settings, vertically or obliquely oriented hyperreflective bands arise within the ONL as the photoreceptor layer buckles over residual SRF. Proposed mechanisms include residual SRF trapped between photoreceptors and RPE, differential slippage or reapposition of outer versus inner retina during reattachment, and biomechanical instability due to hydration[24] or osmotic[22] shifts in the photoreceptor layer. Although ORFs after retinal detachment are often larger and more globular,[25] the same principles likely apply in type 2 CNV: focal exudation in the subretinal space, tethering of the outer retina to the neovascular membrane, and localized buckling under tension.

The consistent disappearance of the pitchfork sign after anti-VEGF therapy strengthens this interpretation. As the neovascular complex regressed and the subretinal space collapsed beneath a newly formed PED,[9] the outer retina flattened, folds resolved, and no recurrent pitchfork patterns were observed. Other contributory factors cannot be excluded but were beyond the scope of this analysis.

This study has limitations. It is retrospective and single center. Imaging quality varied over the 10-year inclusion period, and full volumetric reconstruction was not available in all eyes. Indocyanine green angiography was not systematically obtained, so low-grade choroidal inflammation cannot be completely excluded. Functional testing beyond BCVA, such as microperimetry or multifocal electroretinography, was not available, limiting structure−function interpretation. Finally, although we defined recurring fold morphologies (open, gentle, tight, closed), we did not assess intergrader agreement or determine whether these represent sequential stages versus concurrent patterns.

In summary, the pitchfork sign in type 2 CNV reflects transient mechanical folding and splitting of the outer retina at the interface between subretinal neovascular tissue and the neurosensory retina. It is not specific for inflammatory neovascularization. Clinically, the presence of a pitchfork sign alone should not be used to label a lesion as "inflammatory CNV" or to justify immunosuppression without appropriate inflammatory workup and multimodal imaging. The prompt disappearance of the sign after anti-VEGF therapy, and its association with worse presenting vision, suggest that it marks acute biomechanical stress on the outer retina and represents a potentially reversible target of timely treatment.

Declaration of Generative AI and AI-Assisted Technologies in the Writing Process

During the preparation of this work, the authors used ChatGPT5 to improve readability and language of the manuscript. After using this tool/service, the authors reviewed and edited the content as needed and took full responsibility for the content of the publication.

Footnotes and Disclosures

Originally received: November 15, 2025.
Final revision: March 4, 2026.
Accepted: April 10, 2026.
Available online: April 21, 2026. Manuscript no. XOPS-D-25-01004.

[1] Department of Ophthalmology, IRCCS San Raffaele Scientific Institute, Milan, Italy.

[2] School of Medicine, Vita-Salute San Raffaele University, Milan, Italy.

[3] NIHR Biomedical Research Centre, Moorfields Eye Hospital NHS Foundation Trust and UCL Institute of Ophtalmology, London, United Kingdom.

[4] Department of Optometry and Visual Science, City St George's, University of London, London, United Kingdom.

Disclosure(s):

All authors have completed and submitted the ICMJE disclosures form.

The author(s) have made the following disclosure(s):

G.O.: Consultant − Alcon Inc; Stock or stock options − Relayer Ltd.

F.B.: Consultant − Allergan Inc, Bayer Shering-Pharma, Hoffmann-La-Roche, Novartis, Sanofi-Aventis, Thrombogenics, Zeiss, Boehringer-Ingelheim, Fidia Sooft, Ntc Pharma, Sifi.

Support for Open Access publication was provided by the IRCCS San Raffaele Scientific Institute

HUMAN SUBJECTS: Human subjects were included in this study. The Institutional Review Board of the San Raffaele Scientific Institute approved the study. All research adhered to the tenets of the Declaration of Helsinki. Written informed consent was waived by the local institutional review board due to the retrospective design of the study.

No animal subjects were used in this study.

Author Contributions:

Conception and design: Balduzzi, Ometto, Miserocchi

Analysis and interpretation: Balduzzi, Ometto, Bandello, Miserocchi, Cicinelli

Data collection: Balduzzi, Cicinelli

Obtained funding: N/A

Overall responsibility: Balduzzi, Ometto, Bandello

Abbreviations and Acronyms:
3D = 3-dimensional; **BCVA** = best-corrected visual acuity; **CNV** = choroidal neovascularization; **ELM** = external limiting membrane; **EZ** = ellipsoid zone; **OCTA** = OCT angiography; **ONL** = outer nuclear layer; **PED** = pigment epithelial detachment; **RPE** = retinal pigment epithelium; **SHRM** = subretinal hyperreflective material; **SRF** = ubretinal fluid.

Keywords:
Pitchfork sign, Type 2 choroidal neovascularization, OCT, En face OCT, 3D reconstruction.

Correspondence:
Maria Vittoria Cicinelli, MD, Department of Ophthalmology, IRCCS San Raffaele Scientific Institute, Via Olgettina 60, Milan 20132, Italy. E-mail: Cicinelli.mariavittoria@hsr.it.

References

1. Hoang QV, Cunningham Jr ET, Sorenson JA, Freund KB. The "pitchfork sign" a distinctive optical coherence tomography finding in inflammatory choroidal neovascularization. *Retina*. 2013;33:1049–1055.
2. Pandya BU, Grinton M, Mandelcorn ED, Felfeli T. Retinal optical coherence tomography imaging biomarkers: a review of the literature. *Retina*. 2024;44:369–380.
3. Rajabian F, Arrigo A, Grazioli A, et al. Focal choroidal excavation and pitchfork sign in choroidal neovascularisation associated with choroidal osteoma. *Eur J Ophthalmol*. 2021;31:NP67–NP70.
4. Ramtohul P, Comet A, Denis D. The pitchfork sign: a novel OCT feature of choroidal neovascularization in tuberculosis. *Ophthalmol Retina*. 2019;3:615.
5. Christakopoulos C, Munch IC. The "pitchfork sign" on optical coherence tomography in a case of acute syphilitic posterior placoid chorioretinitis. *Acta Ophthalmol*. 2019;97:e942–e943.
6. Gao R, Ma J, Zhang Z, et al. Spectral domain-optical coherence tomography retinal biomarkers in choroidal neovascularization of multifocal choroiditis, myopic choroidal neovascularization, and idiopathic choroidal neovascularization. *Ann Med*. 2021;53:1270–1278.
7. Gelormini F, Parisi G, Vallino V, et al. Pitchfork sign following pars plana vitrectomy for idiopathic epiretinal membrane: a case report. *Eur J Ophthalmol*. 2024;34:NP92–NP96.
8. Falavarjani KG, Au A, Anvari P, et al. En Face OCT of Type 2 Neovascularization:A Reappraisal of the Pitchfork Sign. *Ophthalmic Surg Lasers Imaging Retina*. 2019;50:719–725.
9. Dolz-Marco R, Phasukkijwatana N, Sarraf D, Freund KB. Regression of type 2 neovascularization into a type 1 pattern after intravitreal anti-vascular endothelial growth factor therapy for neovascular age-related macular degeneration. *Retina*. 2017;37:222–233.
10. Montolio-Marzo S, Pinazo RG, Palacios-Pozo E, Dolz-Marco R. New method to facilitate tomographic macular neovascularization classification in age-related macular degeneration. *Ophthalmic Surg Lasers Imaging Retina*. 2025;56:540–544.
11. Ramtohul P, Malcles A, Gigon E, et al. Long-term outcomes of bacillary layer detachment in neovascular age-related macular degeneration. *Ophthalmol Retina*. 2022;6:185–195.
12. Cicinelli MV, LTDF E, La Franca L, et al. Risk factors of vision loss and multiple recurrences in myopic macular neovascularization. *Retina*. 2023;43:275–285.
13. Marchese A, Giuffre C, Cicinelli MV, et al. The identification of activity of choroidal neovascularization complicating angioid streaks. *Eye (Lond)*. 2022;36:1027–1033.
14. Parodi MB, Cicinelli MV, Marchese A, et al. Intravitreal aflibercept for management of choroidal neovascularization secondary to angioid streaks : the Italian EYLEA-STRIE study. *Eur J Ophthalmol*. 2021;31:1146–1153.
15. Dolz-Marco R, Fine HF, Freund KB. How to differentiate myopic choroidal neovascularization, idiopathic multifocal choroiditis, and punctate inner choroidopathy using clinical and multimodal imaging findings. *Ophthalmic Surg Lasers Imaging Retina*. 2017;48:196–201.
16. Cicinelli MV, Menean M, Apuzzo A, et al. Presumed Müller cell activation in multiple evanescent white dot syndrome. *Invest Ophthalmol Vis Sci*. 2023;64:20.
17. Feo A, Ramtohul P, Govetto A, et al. En face OCT: breakthroughs in understanding the pathoanatomy of retinal disease and clinical applications. *Prog Retin Eye Res*. 2025;106:101351.
18. Cicinelli MV, Giuffre C, Marchese A, et al. The bacillary detachment in posterior segment ocular diseases. *Ophthalmol Retina*. 2020;4:454–456.
19. Ramtohul P, Engelbert M, Malcles A, et al. Bacillary layer detachment: multimodal imaging and histologic evidence of a novel optical coherence tomography terminology: literature review and proposed theory. *Retina*. 2021;41:2193–2207.
20. Zicarelli F, Azzolini C, Cornish E, et al. Optical coherence tomography features of choroidal neovascularization and their correlation with age, gender, and underlying disease. *Retina*. 2021;41:1076–1083.
21. Gupta RR, Iaboni DSM, Seamone ME, Sarraf D. Inner, outer, and full-thickness retinal folds after rhegmatogenous retinal detachment repair: a review. *Surv Ophthalmol*. 2019;64:135–161.
22. Muni RH, Darabad MN, Oquendo PL, et al. Outer retinal corrugations in rhegmatogenous retinal detachment: the retinal pigment epithelium-photoreceptor dysregulation theory. *Am J Ophthalmol*. 2023;245:14–24.
23. Dhewale S, Kelgaonkar A, Khalsa A, et al. Clinical and imaging characteristics of outer retinal folds in eyes with retinitis. *Indian J Ophthalmol*. 2022;70:2981–2985.
24. Dalvin LA, Spaide RF, Yannuzzi LA, et al. Hydration folds in rhegmatogenous retinal detachment. *Retin Cases Brief Rep*. 2020;14:355–359.
25. dell'Omo R, Tan HS, Schlingemann RO, et al. Evolution of outer retinal folds occurring after vitrectomy for retinal detachment repair. *Invest Ophthalmol Vis Sci*. 2012;53:7928–7935.